X-Ray and Magnetization Studies of Cr-Modified Mn_2Sb

F. J. DARNELL, W. H. CLOUD, AND H. S. JARRETT
Central Research Department, E. I. du Pont de Nemours and Company, Wilmington, Delaware*
(Received 3 December 1962)

The three magnetic states which occur in the Cr-modified Mn_2Sb system have been studied by measurements of magnetization, torque, and x-ray lattice cell dimension on single crystals. The exchange inversion transitions between magnetic states for a given composition are shown by x ray to be first order. The field dependence of magnetization allows differentiation of the three magnetic states which exhibit ferrimagnetic, intermediate, and antiferromagnetic spin configurations. Torque and magnetization measurements show that for both the ferrimagnetic and antiferromagnetic states there is a change from positive to negative uniaxial anisotropy with decreasing temperature.

INTRODUCTION

THE ferrimagnetic compound Mn_2Sb can be modified with chromium to form compositions $Mn_{2-x}Cr_xSb$, with $0.01<x<0.25$. These compositions show the unusual magnetic sequence ferrimagnetic $\rightarrow$ antiferromagnetic, without change in crystal structure, as the temperature decreases.[1,2] The exchange transition between the two magnetic states is first order, and may be obtained at any temperature from 140 to 400°K by adjustment of the chromium content. For compositions with transitions below 140°K two first-order transitions occur, ferrimagnetic $\rightarrow$ intermediate $\rightarrow$ antiferromagnetic; for transitions below $\sim$100°K the second transition is not observed down to 4°K. Conditions under which such first-order magnetic transformations can occur have been shown by Kittel[3] to arise when the magnetic exchange interaction is coupled with the elastic strain of the lattice, and when the net exchange is zero for some critical value of the lattice parameter that is attainable by variation in temperature. The role of chromium substitution for manganese in the present system is to contract the Mn_2Sb lattice so that the critical dimension is thermally achieved.[4] Since the net-exchange interaction goes through zero, it is small for temperatures in the neighborhood of the transition temperature. The system, then, is one in which applied fields become comparable to the internal exchange field even at temperatures of a few hundred degrees Kelvin; the effect of such applied fields and of comparable anisotropy fields on the magnetization and spin configurations yields information about the exchange.

This paper presents detailed data on magnetization, crystalline anisotropy, and x-ray parameters, and discusses these results on the basis of molecular field theory.

MATERIALS

The compositions were generally made by fusion of the elements as powders in the desired proportions under argon to form a melt from which crystals could be pulled by the Czochralski technique. Pulling rates of $\frac{1}{2}$ in./h were used, and the seed crystals were commonly oriented so that a tetragonal a axis corresponded to the growth direction. Various thermal treatments were used on polycrystalline compositions to provide more homogeneous materials, but the single crystals were in general not further treated. In all of the samples a second phase of MnSb was present as a Widmanstätten precipitate[5] in amounts of 0.5 to 3% by volume. In some samples, small amounts of manganese were present as a third phase.[5]

The chromium content through a sample varies somewhat as shown by electron-probe measurements, with segregation of Cr into second-phase regions where the ratio of Cr to Mn may be twice that in the matrix Mn_2Sb. Little chromium variation was found within the matrix except close to second phases. The chromium contents reported are the charge compositions, which are in agreement with wet chemical determinations on the final materials. Such analyses obviously give only an average chromium content and neglect the variations in distribution over the different phases. However, these chromium concentrations are believed to represent a reasonable measure of the Mn_2Sb-phase chromium content and have proven useful as a parameter to designate the modification of Mn_2Sb. It should be borne in mind that samples of high Cr content, $x\sim0.15$, with the same nominal composition, may vary in transition temperature by as much as 40°K, and the transition of a given sample may take place over a temperature interval of $\sim$4 to 20°K, presumably because of chromium variations. Crystal orientation for most magnetic studies was achieved by making use of cleavage parallel to the a-a plane of the Mn_2Sb tetragonal structure.

CRYSTAL STRUCTURE STUDIES

A full discussion of the space group and atomic positions of Mn_2Sb and $Mn_{2-x}Cr_xSb$ is given in a paper[6]

[1] T. J. Swoboda, W. H. Cloud, T. A. Bither, M. S. Sadler, and H. S. Jarrett, Phys. Rev. Letters 4, 503 (1960).
[2] W. H. Cloud, H. S. Jarrett, A. E. Austin, and E. Adelson, Phys. Rev. **120**, 1969 (1960).
[3] C. Kittel, Phys. Rev. **120**, 335 (1960).
[4] T. A. Bither, P. H. L. Walter, W. H. Cloud, T. J. Swoboda, and P. E. Bierstedt, Suppl. J. Appl. Phys. **33**, 1346 (1962).
[5] J. D. Wolf and J. E. Hanlon, J. Appl. Phys. **32**, 2584 (1961).
[6] A. E. Austin, E. Adelson, and W. H. Cloud (to be published).

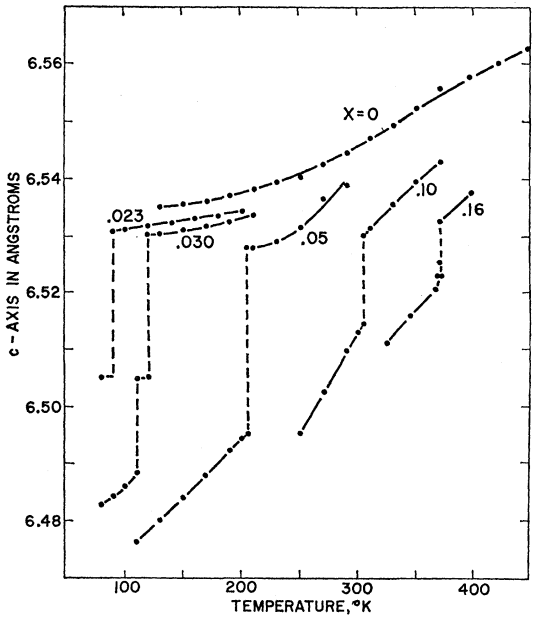

FIG. 1. X-ray c-axis vs temperature; for $Mn_{2-x}Cr_xSb$; data on cooling.

on neutron diffraction. The following points are of importance here: (1) $Mn_{2-x}Cr_xSb$, $0.01 \leq x \leq 0.25$, has the same space group as Mn_2Sb. (2) The space group does not change at the exchange transition. (3) Cr substitutes for Mn randomly in the Mn(I) positions.

X-ray cell parameters were measured using small single crystals weighing less than 1 mg. A General Electric XRD-5 diffractometer with single-crystal orienter was used. In order to achieve the highest possible accuracy, the reflections were taken at the largest observable Bragg angles ($130° < 2\theta < 150°$). The crystal temperature was varied from room temperature

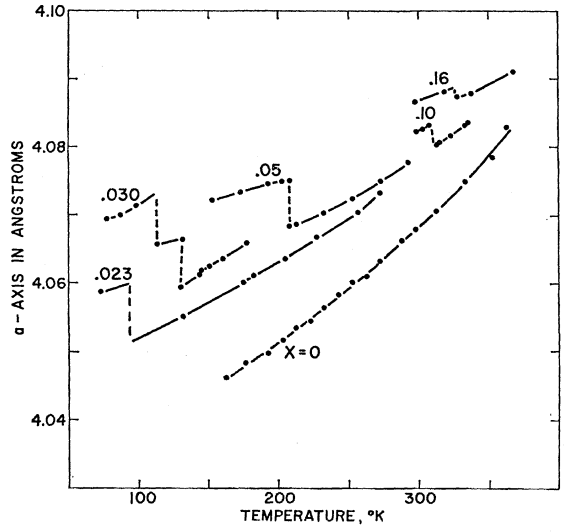

FIG. 2. X-ray a-axis vs temperature; for $Mn_{2-x}Cr_xSb$; data on cooling.

to 77°K using a flow of cooled nitrogen. The method is similar to that described by Post *et al.*[7]

For measurements above room temperature the crystals were heated using a stream of warmed nitrogen.

At the high Bragg angles a resolution of less than one-tenth of the Mo $K\alpha_2$ separation was obtained, giving relative accuracies of c and a to better than 0.0005 Å for any given specimen. Since the C face is a natural cleavage face, the crystal geometry is better suited to accurate measurements of c than of a. We estimate an absolute error of less than 0.001 Å for c and slightly greater than 0.001 Å for a.

The temperature dependence of the c axis is shown in Fig. 1 with the chromium content x as a parameter. For $x=0$, the values obtained in the present measurements show the temperature dependence reported by Heaton and Gingrich,[8] but are systematically smaller than their values over the entire temperature range. The present d values obtained from single crystals were checked by dusting tungsten powder on the a-a plane of a crystal and using the accurately known d values of tungsten as internal standards. As x increases from zero, the room-temperature c axis becomes smaller, and with further change upon cooling reaches a critical value at which an abrupt contraction of the lattice takes place. For sufficiently high values of x, this transition occurs above room temperature. Figures 1 and 2 also show that for low values of x, a single first-order transition to an intermediate c-axis value may take place, or two first-order transitions may occur for a given composition with change in temperature. The magnetic properties of the three states are discussed below. The transitions show thermal hysteresis so that the transition observed on cooling is at a lower temperature than the corresponding transition upon warming. This effect becomes more pronounced at the lowest temperatures where the hysteresis is about 20° at 70°K. Figure 3 shows the hysteresis as observed by magnetization measurements.

TABLE I. Lattice changes at exchange transitions.

	T_s (°K)	$10^3\Delta c/c$	$10^3\Delta a/a$
F/AF	375	1.07	···
	323	···	0.34
	308	2.40	0.60
	290	2.82	···
	200	4.60	2.03
	125[a]	6.22	3.00
F/I	133	3.76	1.49
	131	···	1.81
	123	3.83	···
	88	3.93	1.94
I/AF	113	2.52	1.53
	105	···	1.75

[a] Sum of F/I and I/AF changes, with an average T_s.

[7] B. Post, R. S. Schwartz, and I. Fankuchen, Rev. Sci. Instr. **22**, 218 (1951).

[8] L. Heaton and N. S. Gingrich, Acta Cryst. **8**, 205 (1955).

While the c axis is undergoing a discontinuous contraction, the a axis is expanding as shown in Fig. 2, so that the net-volume change remains small. The discontinuous changes Δc and Δa are given in Table I for several transition temperatures.

MAGNETIZATION

Measurements of the magnetic moment were made with a pendulum magnetometer with the sample in a uniform gradient field with average fields from 2500 to 16 750 Oe. A strain-gauge transducer was used to measure force exerted on the sample. An accuracy of 0.1 emu/g was obtained for the usual 0.1-g crystal sample. Temperatures from 20 to 600°K were obtained

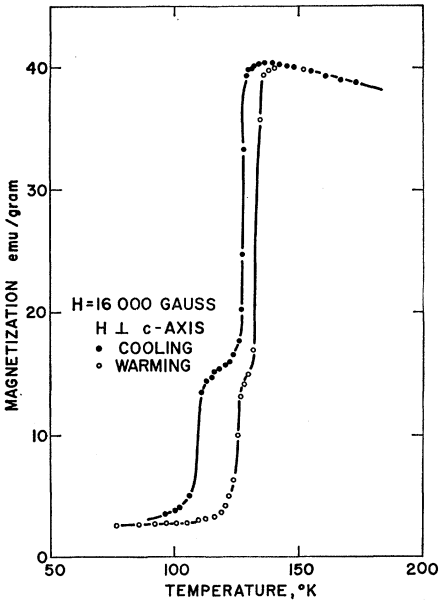

FIG. 3. Magnetization vs temperature for $Mn_{1.97}Cr_{0.03}Sb$; data on cooling and warming to demonstrate hysteresis. $H \perp c$.

by flow of cooled or heated gases past the sample. A second method employing a ballistic magnetometer was used to study magnetization in fields from 0 to 4000 Oe and at temperatures down to 1.8°K.

Measurements of magnetization as a function of field showed samples in the ferrimagnetic state to be within 0.5% of saturation at 16 000 Oe for all temperatures. The temperature dependence of saturation magnetization for samples with several chromium contents are shown in Fig. 4. The saturation moment of Mn_2Sb extrapolated to 0°K is 40.0 emu/g, subtracting a moment of 2.0 emu/g for MnSb. The Curie point was determined to be 565°K; this is above the value 550°K found by Guillaud.[9] Our moment for Mn_2Sb lies somewhat below the saturation value of 45.2 emu/g of Guillaud. If correction for MnSb is not made, the difference becomes smaller. We suspect that the higher value observed by Guillaud may have arisen from small

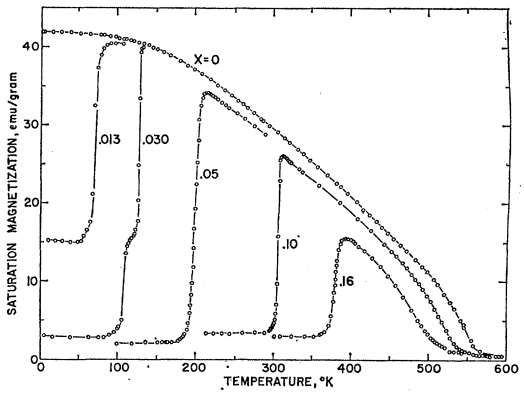

FIG. 4. Magnetization vs temperature; for $Mn_{2-x}Cr_xSb$; data on cooling; $H \perp c$.

additional amounts of MnSb which has a saturation moment of 111.8 emu/g.[9] As chromium is added, the Curie temperature decreases monotonically, and the saturation moment at a given temperature also decreases. On a plot of reduced magnetization vs reduced temperature, data for all of the samples fall very close to the same curve. The magnetic state above the transition temperature T_s is ferrimagnetic (F), just as in Mn_2Sb. The low moment state, as confirmed by neutron diffraction[2] is antiferromagnetic (AF), while the intermediate (I) state found at low temperatures possesses a more complex spin arrangement.[6]

The three magnetic states may be differentiated by measurement of the field dependence of magnetization.[10] In the ferrimagnetic state saturation is obtained in the easy direction at fields less than 1000 Oe. The field required for saturation in the hard direction gives a measure of the crystalline anisotropy which is in agreement with the direct anisotropy measurements below.

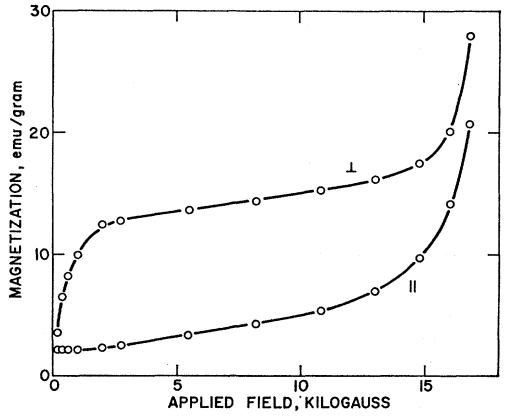

FIG. 5. Magnetization vs magnetic field for $Mn_{1.97}Cr_{0.03}Sb$; in the intermediate state. ⊥ and ‖ designate direction of field with respect to c axis.

[9] C. Guillaud, thesis, University of Strasbourg, 1943 (unpublished).

[10] P. E. Bierstedt, F. J. Darnell, W. H. Cloud, R. B. Flippen, and H. S. Jarrett, Phys. Rev. Letters 8, 15 (1962).

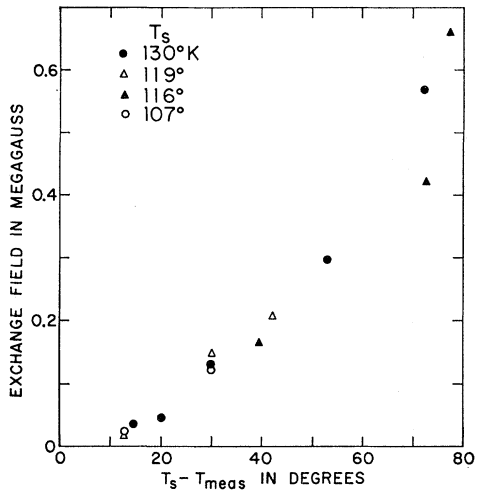

FIG. 6. Exchange field (calculated from susceptibility) vs $T_s - T_{meas}$.

The change of the easy direction at $-30°$C from parallel to c to perpendicular to c is in agreement with the observations of Guillaud.

Magnetization for a sample in the intermediate state is shown in Fig. 5 for magnetic fields applied parallel and normal to the c axis. The initial magnetization curve for the intermediate state with the field applied normal to the c axis shows saturation effects similar to the domain effects of the ferrimagnetic state. It is concluded from this that the intermediate state possesses a zero-field magnetic moment intermediate between those of the ferri- and antiferromagnetic states. For fields parallel to the c axis, even up to 16 000 Oe, this moment is not seen. From this it is concluded that the magnetization of the intermediate state lies in the a-a plane and that the state possesses a crystalline anisotropy much higher than $\sim$16 000 Oe. The magnetization as a function of field above $\sim$1000 Oe is linear for both orientations of field so that an effective susceptibility is determined. From the susceptibility normal to the c axis, it is possible to calculate the exchange field constant $\lambda = 1/\chi_\perp$ and the exchange field $H_E = \lambda M$, where M is the sublattice magnetization. Values of the exchange field so calculated are shown as a function of $T_s - T$ in Fig. 6. As expected,[3] they extrapolate to a small value, $\sim$10 000 Oe, at the transition temperature. The anisotropy field H_A may be estimated from the extrapolated intersection of the magnetization curves for the two field orientations. This gives values of 30 000 to 80 000 Oe, depending mainly on the temperature of measurement. These are of the order predicted by the expression $H_A = 2K/M$ if we use K appropriate to the ferrimagnetic state of Mn_2Sb at the corresponding temperature and M appropriate to the intermediate state. At very high fields the abrupt increase in magnetization observed is due to a transition to the ferrimagnetic state caused by the applied field.

In the antiferromagnetic state it should again be possible to determine H_E from the field dependence of magnetization. However, observation of this dependence is obscured by the presence of the ferromagnetic MnSb, particularly at temperatures much below the transition temperature. In spite of this second phase, an anisotropy inversion temperature T_A for the antiferromagnetic case can be determined for samples with high chromium content by comparison of the temperature dependence of magnetization measured parallel or normal to the c axis at temperatures just below T_s. Most compositions in the antiferromagnetic state exhibit negative uniaxial anisotropy so that a larger susceptibility or moment is measured for H normal to c than for H parallel to c. For compositions with $T_s > 80°$C, the relative susceptibilities for the two field directions reverse at a temperature below T_s, indicating a change in the crystalline anisotropy to positive uniaxial with increasing temperature. The locus of these transitions is shown in Fig. 10.

CRYSTALLINE ANISOTROPY

Anisotropy measurements were obtained from analysis of torque curves by the standard technique of comparing the experimental data to the equilibrium expression for the torque exerted on the magnetic moment,

$$T = \partial E/\partial\phi = HM\sin(\theta-\phi) - 2K_1\sin\phi\cos\phi - 4K_2\sin^3\phi\cos\phi = 0, \quad (1)$$

where H is the internal field $H_0 - NM$, M is the saturation magnetization at a given temperature, and θ and ϕ are the angles formed by the c axis with H and M, respectively.

Single-crystal samples of Mn_2Sb were cut in the shape of disks containing the tetragonal a-c plane in the plane of the disk. The samples were then rotated about the second a axis on a torque magnetometer designed after that of Byrnes and Crawford.[11] In this design, the sample is attached to a rigid shaft mounted in nonmagnetic bearings, and the torque is converted by a suitable linkage into a linear force and measured by strain-gauge transducers. A torque range of 80 to 8×10^4 dyn cm could be measured with this apparatus. The torque was determined as a function of temperature in a constant applied field of 16 900 Oe. Temperatures from 20 to 515°K were obtained by blowing cooled or heated air through a Dewar containing the sample and shaft or by use of low-temperature baths. K_1 and K_2 were determined from a least-squares fit of the theoretical torque expression to the data.

The anisotropy results for Mn_2Sb are shown in Fig. 7 and agree qualitatively with those of Guillaud. K_1 shows a peak at 410°K of 75×10^4 ergs/cm^3, considerably

[11] W. S. Byrnes and R. G. Crawford, J. Appl. Phys. **29**, 493 (1958).

higher than the maximum estimated from Guillaud's data.

As chromium is substituted in Mn_2Sb, the general form of the temperature dependence is retained, but a family of curves is formed with a gradual decrease in the transition temperature T_A and a slight increase in the maximum positive value of K_1. The values of K_2 could not be accurately determined because of the presence over most of the range of the much larger first-order anisotropy. The compensation point $-K_1=K_2$ occurs at 247°K, in contrast to Guillaud's value of 240°K; $K_1=0$ at 250°K and $-K_1=2K_2$ at 244°K. In this range, $0>K_1>-2K_2$, the easy direction of magnetization changes continuously from the c axis at high temperature to the (001) plane at low temperatures. The limits of this temperature range are in exact agreement with the transition as determined by neutron diffraction.[12]

Torque measurements were made in the a-a plane for three samples of Mn_2Sb and four of Cr-modified Mn_2Sb. The observed anisotropies varied from the limit of sensitivity (0.5×10^4 ergs/cm³) to values of $K_3\sim5\times10^4$ ergs/cm³, where a possible basal plane anisotropy $K_3\sin^2\psi\cos^2\psi$ was assumed. In some samples torques of 180° symmetry were found which decreased monotonically over the range −100 to 100°C. It is believed that all of these basal plane torques arise from a second phase of MnSb which has been shown[13] to precipitate in (101) planes of the Mn_2Sb structure and is usually present to the extent of a few percent. MnSb has a large anisotropy, $\sim1\times10^6$ ergs/cm³, which is independent of temperature, and a fairly high magnetization; less than 2% by volume of MnSb is sufficient to account for the observed torques. If the torque is assumed to arise from an Mn_2Sb anisotropy of the form noted above, values of $K_3\sim3\times10^4$ ergs/cm³ are obtained in agreement with the value 3.4×10^4 ergs/cm³ reported by Guillaud[9] for room temperature. Guillaud reports a change in sign of K_3 at −33°C which we would not find in such an interpretation of our torque results. We conclude that in pure Mn_2Sb there is little or no basal plane anisotropy, $K_3<0.5\times10^4$ ergs/cm³, and that observed torques in the a-a plane are due to small amounts of MnSb precipitate.

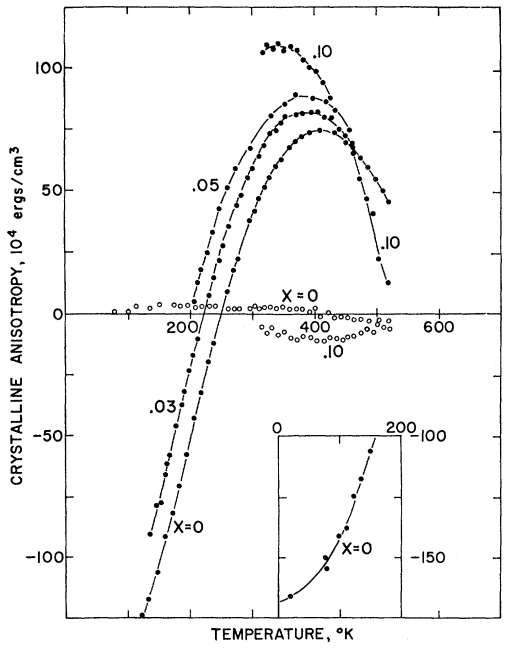

FIG. 7. Crystalline anisotropy energy coefficients K_1 (dots) and K_2 (open circles) vs temperature for $Mn_{2-x}Cr_xSb$.

Measurements by the torque technique are not possible for the antiferromagnetic state, and no meaningful values can be obtained for the intermediate state because of the complex dependence of magnetization on field and orientation. As indicated above, values of the anisotropy field H_A determined from magnetization measurements indicate values of K for the intermediate state comparable with those of the ferrimagnetic state. By comparison of the ferrimagnetic anisotropy values with the antiferromagnetic spin orientations as observed by neutron diffraction, it is seen that associated with the transition to the antiferromagnetic state is a substantial negative contribution to the uniaxial anisotropy. For a composition with $T_s\simeq400$°K, the ferrimagnetic anisotropy just above T_s is $\sim80\times10^4$ ergs/cm³, while the antiferromagnetic anisotropy just below T_s is negative.

DISCUSSION

Magnetization

Néel[14] has calculated the magnetization curve of Mn_2Sb, using molecular field constants derived from susceptibility measurements. Alternatively, a least-squares fit to the magnetization data can be made with the molecular field constants as adjustable parameters.

The molecular field approach to solving magnetic spin-ordering problems is well known, and the notation used by Néel is employed. Mn_2Sb is assumed, for the sake of simplicity, to be comprised of two sublattices, one of Mn(I) sites and one of Mn(II) sites whose saturation magnetic moments are $M_j=NgJ\beta_0$ and $M_k=NgK\beta_0$, respectively. The magnetization at site I is given by the usual Brillouin function

$$M_I=M_jB_j(M_jH_I/RT), \tag{2}$$

where

$$H_I=n(\alpha\lambda M_I+\mu M_{II}) \tag{3}$$

is the effective molecular field at site I for antiferromagnetic coupling between sites I and II. The fractions

[12] M. K. Wilkinson, N. S. Gingrich, and C. G. Shull, J. Phys. Chem. Solids 2, 289 (1957).

[13] We are indebted to Dr. J. J. Cox of the Du Pont Engineering Research Laboratory for this finding and for several discussions.

[14] L. Néel, Ann. Phys. (N. Y.) 3, 137 (1948).

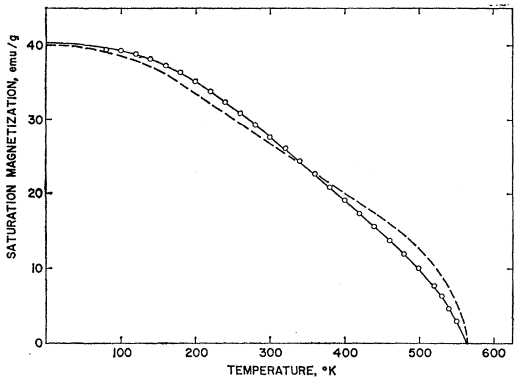

FIG. 8. Magnetization vs temperature for Mn_2Sb. Circles represent experimental data; Néel's and the present molecular field magnetizations are shown by the dashed and solid lines, respectively.

of magnetic ions occupying sites I and II are λ and μ, respectively, and $n\alpha$ and n are the molecular field constants. Expressions similar to Eqs. (2) and (3) also hold for site II with $n\beta$ as the molecular field constant between Mn(II) sites. Solution for the sublattice magnetizations may be obtained numerically by methods proposed by Néel or by Rado and Folen.[15] These methods are, however, laborious and time consuming and may be performed more readily on a computer, especially when attempting a least-squares fit. The molecular field constant n is determined from the Curie temperature T_c by the relation,

$$\left(\frac{T_c}{n}\right)\frac{2T_c}{n}(\beta\mu C_k+\lambda\alpha C_j)+C_jC_k\lambda\mu(\alpha\beta-1)=0, \quad (4)$$

for a given α and β, where $C_k=(k+1)M_k^2/3kR$ and $C_j=(j+1)M_j^2/3jR$ are the Curie constants for the two manganese sites. We take $j=\frac{3}{2}$ and $k=\frac{5}{2}$ as giving the best agreement with high-temperature susceptibility data.

With a Curie temperature of 565°K and $j=3/2$, $k=5/2$, the best fit to the experimental points by the calculated magnetization $M=|\lambda M_{\rm I}-\mu M_{\rm II}|$ is shown as the solid line in Fig. 8; the dashed curve shows Néel's calculated curve. The molecular field constants obtained here are given in Table II with the results of Néel for comparison. To calculate the molecular field constants it is also necessary to select values of g appropriate to the manganese sites. These may be chosen to give the moments $g_{\rm I}j\beta_0$ and $g_{\rm II}k\beta_0$ observed by neutron diffraction (case A, with $g_{\rm I}=1.25$ and $g_{\rm II}=1.42$, in Table II) or chosen to correspond to approximately isotropic spins while retaining agreement with experiment for the ratio $M_{\rm I}/M_{\rm II}$ and the difference $M=|\lambda M_{\rm I}-\mu M_{\rm II}|$, (case B, with $g_{\rm I}=2.06$ and $g_{\rm II}=1.90$). Although the resulting molecular field coefficients are different, the calculated magnetizations as functions of temperature are the same to within 1%. It is seen that α and β not only are larger than those obtained by Néel but are of opposite sign. The positive signs of α and β indicate strong ferromagnetic coupling between like manganese ions. The molecular field solution includes determination of the Mn(I) and Mn(II) sublattice magnetizations. These calculated magnetizations are in good agreement with the neutron diffraction moment measurements.[6]

It should be pointed out here that the molecular field constants are valuable only as a means of representing the magnetization curve by an empirical equation with as few arbitrary parameters as possible. The susceptibility derived from the present molecular field constants is not in close agreement with the experimental points; however, α and β, calculated from susceptibility data obtained in these laboratories, are both positive rather than negative as found by Néel. Their lack of significance can further be seen by taking two different values of j and k, namely, 1 and 2, and again making a least-squares fit to the experimental points. The fit to the magnetization is just as good as the one obtained above, but the α, β, and n shown in Table II (case C) are quite different. We, therefore, regard this agreement between theoretical and experimental magnetization as largely fortuitous. As we shall see below, calculations of crystalline anisotropy are much more sensitive to choice of spins and g values, and agreement with experiment is found only for $j=3/2$, $k=5/2$ and $g_{\rm I}=1.30$ and $g_{\rm II}=1.48$.

Molecular field calculations for the chromium-modified samples were also carried out. Although different values of the molecular field constants n, α and β are needed, there are no changes in sign which would indicate a reversal in one of the three exchanges in the two-sublattice model. These calculations are, of course, inconclusive for at least three reasons. First, we are fitting only the data for the ferrimagnetic state where the exchange interactions might be expected to remain very similar to those of Mn_2Sb. Second, a two-sublattice model is not adequate to explain the more complex spin configurations of the intermediate state and therefore might not be expected to prove fruitful. Third, and probably most important, the molecular-

TABLE II. Molecular field coefficients.

	j	k	n	α	β
For Mn_2Sb					
Néel[a]	5/2	3/2	526	−0.24	−0.20
Present work–A	5/2	3/2	144.3	+0.56	+2.72
–B	5/2	3/2	61.7	0.89	2.28
–C	2	1	148.9	0.44	1.93
For $Mn_{2-x}Cr_xSb$					
$x=0.03$	2	1	216.2	0.04	0.83
$x=0.05$	2	1	187.8	0.23	1.25
$x=0.10$	2	1	164.6	0.42	1.70
$x=0.16$	2	1	87.8	1.44	4.54

[a] See reference 14

[15] G. T. Rado and V. J. Folen, J. Appl. Phys. **31**, 62 (1960).

field treatment assumes temperature-independent exchange fields, while in the present systems it is the variation of exchange with temperature which leads to the unusual properties.

Crystalline Anisotropy

Relative to other uniaxial ferrimagnetic materials[9,16] the anisotropy in Mn_2Sb is low by an order of magnitude. Among the possible sources of anisotropy are dipole-dipole interactions, crystal field effects, anisotropic g values, and anisotropy of exchange. We consider first the dipole contribution. For a calculation of the first-order anisotropy K_1, we are interested in only the first-order energy between two dipoles i and j referred to the x, y, z axes of the unit cell

$$V_{ij}=-\frac{3}{2}\frac{M_iM_j}{N_iN_j}\frac{1}{r_{ij}^5}(3z_{ij}^2-r_{ij}^2)\sin^2\theta,$$

where θ is the angle between the direction of the magnetization and the z axis of the crystal and N is the number of i (or j) sites per unit volume.

We obtain the anisotropy energy per unit volume at dipole i by summing V_{ij} over all j lattice sites and multiplying by 1/2 to correct for counting each interaction twice

$$K_i=-\frac{3}{4}M_i\sum_j\frac{M_j}{N_j}\frac{1}{r_{ij}^5}(3z_{ij}^2-r_{ij}^2).$$

The sum over j may be divided into a sum over Mn(I) sites and a sum over Mn(II) sites. The origin of these sums is assumed to be at site I for the calculation of $K_{\rm I}$, the anisotropy of site I, and at site II for $K_{\rm II}$, the anisotropy of site II.

For the anisotropy of site I we have the sum

$$\sum_i=\frac{M_{\rm I}}{c^3}\sum_{\rm I,I}+\frac{M_{\rm II}}{c^3}\sum_{\rm I,II},$$

where

$$\sum_{\rm I,I}=\sum_{nmL}\left(\frac{3L^2}{[f(n^2+m^2)+L^2]^{5/2}}-\frac{1}{[f(n^2+m^2)+L^2]^{3/2}}\right)=-104.8,$$

and

$$\sum_{\rm I,II}=2\sum_{KL}\left(\frac{3(L+z_1)^2}{\{2f[(\tfrac{1}{2}+H)^2+K^2]+(L+z_1)^2\}^{5/2}}-\frac{1}{\{2f[(\tfrac{1}{2}+H)^2+K^2]+(L+z_1)^2\}^{3/2}}\right)=-14.2.$$

Here, n and m are integer multiples of the distance from a cell corner to the face center in the basal plane, and H, K, and L are integer multiples of the cell dimensions along the axes x, y, and z. The factor $f=a^2/2c^2=0.195$ is the ratio of cell dimensions, and the parameter $z_1=0.295$ is the fractional position of the Mn(II) site above the basal plane.[8]

[16] J. Smit and H. P. J. Wijn, *Ferrites* (John Wiley & Sons, Inc., New York, 1959).

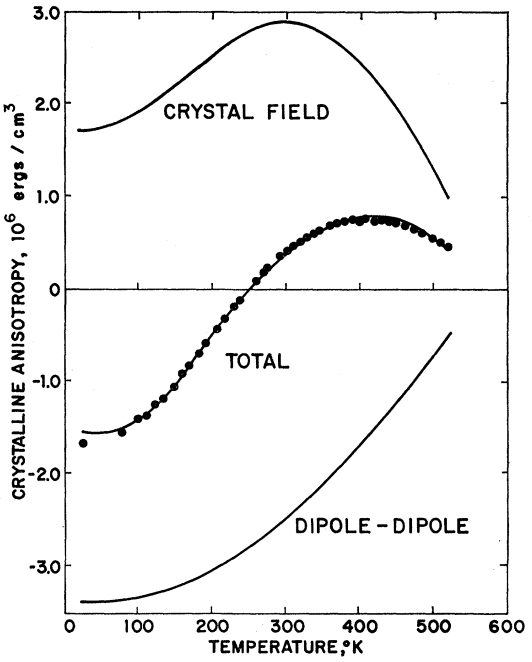

FIG. 9. Crystalline anisotropy energy vs temperature for Mn_2Sb. Circles represent experimental data; upper curve is calculated crystal field energy, lower curve is dipolar energy, and center curve is sum of crystal field and dipolar energies.

Similarly for site II with the origin at $(a/2,\ 0,\ z_1c)$ the sum becomes

$$\sum_i=\frac{M_{\rm I}}{c^3}\sum_{\rm I,II}+\frac{M_{\rm II}}{c^3}\left[\sum_{\rm II,II}^{1}+\sum_{\rm II,II}^{2}\right],$$

where

$$\sum_{\rm II,II}^{1}=\sum_{HKL}\left(\frac{3L^2}{[2f(H^2+K^2)+L^2]^{5/2}}-\frac{1}{[2f(H^2+K^2)+L^2]^{3/2}}\right)=-34.5,$$

$$\sum_{\rm II,II}^{2}=\sum_{HKL}\left(\frac{3(L-2z_1)^2}{\{2f[(\tfrac{1}{2}+H)^2+(\tfrac{1}{2}+K)]+(L-2z_1)^2\}^{5/2}}-\frac{1}{\{2f[(\tfrac{1}{2}+H)2+(\tfrac{1}{2}+K)^2]+(L-2z_1)^2\}^{3/2}}\right)=-10.0.$$

Although the lattice sums will appear in slightly different form for an origin on the second Mn(II) site $[0,\ a/2,\ (1-z_1)c]$ in the unit cell, the sums are identical, as, of course, they must be. The above sums extend from $-\infty$ to $+\infty$. The sums cannot be obtained

analytically and, therefore, were obtained by the direct sum method on an IBM 650 to 20 lattice spacings and a continuum approximation to correct for slow convergence. It is estimated that the sums quoted above are good to the third significant figure.

The dipolar anisotropy energy is then given by

$$K=-\frac{3}{4}\frac{1}{Nc^3}\left[M_{\mathrm{I}}^2\sum_{\mathrm{I,I}}+2M_{\mathrm{I}}M_{\mathrm{II}}\sum_{\mathrm{I,II}}+M_{\mathrm{II}}^2\sum_{\mathrm{II,II}}\right]$$

$=-3.8\times10^6$ ergs/cm^3 at $T=0$ for F ordering, and -3.2×10^6 ergs/cm^3 for AF ordering, for $M_{\mathrm{I}}=2.13$ and $M_{\mathrm{II}}=3.87$ Bohr magnetons. The value extrapolated from the data shown in Fig. 7 is -1.6×10^6 ergs/cm^3, in agreement with Guillaud. It is seen therefore that the calculated dipolar anisotropy for F ordering is too large by a factor of 2.5. It is also apparent that the anisotropy from this source remains negative at all temperatures and decreases monotonically with increasing temperature. The dipolar anisotropy is shown as a function of temperature in Fig. 9.

Although the calculation is based on the molecular field approach, it is believed to represent the dipole-dipole anisotropy because the temperature dependence of the sublattice magnetization agrees well with that measured by neutron diffraction. In any event, the shape and magnitude of the dipolar contribution cannot be altered significantly by reasonable alterations in the temperature dependence of the sublattice magnetization. We cannot, therefore, account for the observed anisotropy by the dipole-dipole energy alone.

The difference between the calculated dipole-dipole energy and the observed anisotropy we attempt to fit by crystal-field contributions. Anisotropy may be expressed to first order in a general analytic form[17]

$$K=DS(S-1/2)(M/M_0)^{\xi}, \tag{5}$$

where $0\leq\xi<3$ is a function of the magnetization but is nearly independent of spin. The upper limit to ξ is the value expected from the Zener theory of anisotropy for complete correlation of spins in which the exponent is $n(n+1)/2$ with $n=2$ for axial symmetry. The decrease of the exponent from 3 at finite temperatures arises from averaging the magnetization over magnetic states where the z component assumes discrete rather than the continuous values of the Zener theory. The functional form of ξ depends on the model selected. Spin dependence, therefore, appears principally as a scale factor which only serves to alter the value of D for different assumed values of the spin.

Wolf[18] has calculated the anisotropy to be expected on an isolated ion model from a weak-crystal-field splitting D of orbitally nondegenerate spin multiplets. His results may be put in the form above, where $2<\xi\leq3$ when the magnetization can be expressed by a Brillouin function. The crystal-field splitting parameter D is unfortunately not calculable because of unknown valence of the manganese ions and also because of unknown screening by the conduction electrons. We may ask, however, what value of D would be needed to fit the experimental results and whether the value obtained is reasonably consistent with other measurements and with known splitting parameters in other substances.

To apply the isolated ion theory of Wolf we must assume the Néel ground state of antiferromagnetically ordered independent Mn ions. For such a model, the total anisotropy is assumed to be the sum of the anisotropies of each sublattice. The functional form of the anisotropy shown in Fig. 9 is obtained only if the crystal-field splitting parameters D_{I} and D_{II} of the two sublattices are of opposite sign.

By use of the Wolf formulation for $S_{\mathrm{I}}=3/2$ and $S_{\mathrm{II}}=5/2$, we adjust g_{I} and g_{II} to give a least-squares fit to the quantity $K_{\text{crystal field}}$, over the range 20 to 520°K. The result of this calculation is shown as the solid line in Fig. 9 where $g_{\mathrm{I}}=1.30$ and $g_{\mathrm{II}}=1.48$. These values are to be compared with the g values of 1.25 and 1.42 required to give the best least-squares fit to the magnetization data. Small variations of g_{I} and g_{II} from their best least-squares value give strong disagreement between experimental anisotropy and theory. Attempts to fit the anisotropy using $j=1$ and $k=2$ were not successful. The mean-square deviation, 4×10^5 ergs/cm^3, of experiment from theory is approximately equal to the estimated experimental accuarcy. The splitting parameters are

$$S_{\mathrm{I}}(S_{\mathrm{I}}-1/2)D_{\mathrm{I}}=1.42\ \mathrm{cm}^{-1}\quad(S_{\mathrm{I}}=\tfrac{3}{2}),$$

$$S_{\mathrm{II}}(S_{\mathrm{II}}-1/2)D_{\mathrm{II}}=-0.33\ \mathrm{cm}^{-1}\quad(S_{\mathrm{II}}=\tfrac{5}{2}).$$

The values of ξ_{I} and ξ_{II} no longer lie within the limits $2<\xi\leq3$, because the magnetization is not a Brillouin function. At low temperature, ξ_{I} and ξ_{II} show the largest deviation from the expected value of 3, being slightly less than 2. At the higher temperatures, they are in agreement with the exponent expected for a Brillouin function. The exponents do not exceed 3, however, for the best fit. For acceptable, but not the best fit, the exponent rises rapidly to a value of the order of 100.

The values obtained for the crystal-field splitting parameters are reasonable for ions in the ionic states assumed and for such ions contained in an insulator. However, these values are probably large for these ions in a good conductor where there is extensive shielding of the crystal field by conduction electrons. It is suspected that the successful fit of theory to experiment is due largely to the fact that axial anisotropy from any source can be represented by Eq. (5) and that it is not the model which is so successful, but the form of the equation.

[17] N. Akulov, Z. Physik **100**, 197 (1936); C. Zener, Phys. Rev. **96**, 1335 (1954); F. Keffer, *ibid.* **100**, 1692 (1955); J. H. Van Vleck, J. Phys. Radium **20**, 128 (1959).

[18] W. P. Wolf, Phys. Rev. **108**, 1152 (1957).

Two additional features of the anisotropy are not explained by this model. First, as chromium is substituted in Mn_2Sb, the anisotropy increases to more positive values. It might be argued that there should be a positive increase in the anisotropy with increasing chromium content because, as neutron diffraction has shown, the magnetization of the Mn(II) ion, which contributes a negative anisotropy, is lowered. However, this decrease in the magnetization is not large enough to account for the observed increase in the anisotropy. Second, the crystal field does not account for the negative AF anisotropy in the temperature region where the F anisotropy is positive. The lattice contraction contributes at most a 1% change in the crystal field and thus is not large enough to account for a negative antiferromagnetic anisotropy over the observed temperature range. Recently, Flippen[19] has confirmed by spin-flopping experiments that the AF anisotropy must be about 10^6 ergs/cm^3 more negative (at least in the narrow temperature range reported).

These large differences in the F and AF anisotropies cannot be accounted for by our present model. We suggest that a third contribution, namely, that of anisotropic exchange, also plays a significant, if not dominant, role in the total anisotropy energy. Preliminary calculations by one of us (HSJ) indicate that anisotropic exchange could account for $K_{\text{crystal field}}$ entirely with no contribution from a crystal-field splitting.

CONCLUSIONS

X-ray studies show that discontinuities characteristic of first-order transitions take place as a function of temperature in compositions of Cr-modified Mn_2Sb. These exchange-inversion transitions are between ordered magnetic states which can be distinguished by their magnetic behavior. In particular, the intersublattice exchange field is determined and is found to approach a value as small as 10 000 Oe at the transition. Magnetic measurements also permit determination of the uniaxial crystalline anisotropy and establishment of the temperature at which it changes from positive to negative. The magnetization and crystalline anisotropy data for Mn_2Sb are treated by molecular-field calculations. Assuming an anisotropy arising from dipole-dipole interactions and crystal-field effects alone, good agreement is obtained with both magnetization and anisotropy data for spins $S_I=3/2$, $S_{II}=5/2$, and g values $g_I\cong 1.30$ and $g_{II}\cong 1.48$.

The several magnetic states and spin configurations observed in the Cr-modified Mn_2Sb system may be conveniently summarized by means of a phase diagram, in Fig. 10. First-order magnetic transitions are indicated by solid lines, the second-order magnetic transition (ferrimagnetic to paramagnetic) by a dashed line, and the anisotropy inversions (defined here as $K_1=0$) by dotted lines.

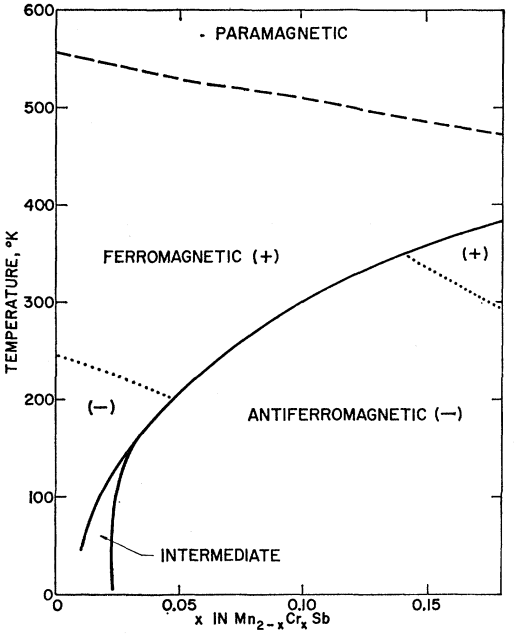

FIG. 10. Phase diagram for the Cr-modified Mn_2Sb system.

Note added in proof. It has come to our attention that Tonegawa[20] has also calculated the temperature dependence of anisotropy energy for Mn_2Sb. He employs the isolated ion model and analyzes the anisotropy in terms of dipolar and crystal field terms, with results qualitatively similar to ours.

ACKNOWLEDGMENTS

We wish to acknowledge the contributions of Dr. A. E. Austin of Battelle Memorial Institute, who performed the electron-probe microanalyses; Professor M. S. Sparks, who carried out the dipole-dipole calculations; Dr. R. B. Flippen, who determined the exchange transition temperatures for several samples and made susceptibility measurements on Mn_2Sb above its Curie temperature; and J. F. Yeninas and K. R. Babcock, who made many of the magnetization and x-ray measurements, respectively.

[19] R. B. Flippen (to be published).

[20] T. Tonegawa, J. Phys. Soc. Japan **17**, 1398 (1962).